

Communication

Mixing and Residence Time Distribution in an Inert Gas-Shrouded Tundish

SAIKAT CHATTERJEE, AMJAD ASAD, CHRISTOPH KRATZSCH, RÜDIGER SCHWARZE, and KINNOR CHATTOPADHYAY

Tracer dispersion experiments were carried out in a multi-strand tundish by injecting 1 (N) NaCl solution into water. The variation of dimensionless concentration–time curves known as C-curves and mixing times with different gas flow rates were studied. The proportions of dead, mixed, and dispersed plug volumes were calculated using the ‘modified mixed model.’ The observations were explained by analyzing the behavior of the bubble plume, incoming jet velocity, and turbulent kinetic energy within the tundish.

DOI: 10.1007/s11663-016-0867-7

© The Minerals, Metals & Materials Society and ASM International 2016

Although the tundish was initially conceptualized as a mere vessel to continuously supply liquid steel to the continuous casting mold, researchers have started to realize its full potential. It is now a well-proven fact that the steel cleanliness can be enhanced by controlling melt flow patterns. Controlling melt flows in the tundish is a topic of interest to most steel makers. Melt flow characterization has been performed through computational fluid dynamics (CFD) simulations, particle image velocimetry (PIV), as well as residence time distribution (RTD) experiments. Residence time is defined as the time a single fluid element spends in the reactor vessel.^[1] RTD is a quick and relatively inexpensive technique to characterize melt flow patterns that can provide us with valuable insights. Significant amount of research has been done on RTD in various types of tundishes using a variety of on-line measurement techniques such as

colorimetry, conductimetry, and spectrophotometry.^[1–4] Interestingly, the amount of work done on analyzing the effect of gas injection on fluid flow characteristics is rather scarce. Sahai and Ahuja^[1] and Chang *et al.*^[5] studied the effects of submerged gas injection and gas bubbling curtains on fluid flow and homogenization, whereas Srivastava and Korla^[6] analyzed the effect of air flow through the shroud on fluid flow patterns. During inert gas-shrouding, there is some inherent entrainment of argon gas into the melt and it forms a bubble plume inside the tundish.^[7–9] The authors believe that this type of bubble plume inside the tundish has a significant effect on the RTD and mixing behavior of the tundish. To prove this point, a simple water model experiment was devised where a 1 (N) NaCl solution was injected, and the total mixing time and change in water conductivity were recorded. The conductivity values were converted into dimensionless concentration and subsequently, the dimensionless concentration versus dimensionless time curves, known as C-curves were derived. A schematic diagram showing the experimental setup for measurement of tracer dispersion is shown in Figure 1. It consisted of a one-third scale tundish, water supply, compressed air supply, syringe for tracer injection, and data acquisition devices. Compressed air was used to simulate argon injections at 0 to 10 pct of steel entry flows.

Data from the conductivity meters for all the cases were processed to obtain normalized C-curves. The dimensionless concentration $C(\theta)$ was plotted against the dimensionless time (θ) as is usually done for a tundish. This procedure is explained in detail in standard text.^[10] The RTD curves for the cases of inner and outer submerged entry nozzles (SENs) of the tundish are depicted in Figures 2(a) and (b), respectively. The variation of the dimensionless concentration with dimensionless time for different gas flow rates can also be clearly noticed. The dimensionless concentration is given by

$$C(\theta) = c_i/c_{\text{avg}}, \quad [1]$$

where c_i is any concentration of tracer in the fluid at the vessel exit and c_{avg} is the average concentration of the tracer when it dissolves in the whole tundish fluid. A ‘ $C(\theta)$ ’ value of greater than unity means the instantaneous concentration of tracer is greater than the average tracer concentration. This implies that tracer proceeds directly toward tundish outlets and does not mix completely with the entire volume of tundish fluid under these conditions, suggesting the presence of dead volumes in the tundish. The RTD curves for both inner and outer SENs under no gas flow show peak $C(\theta)$ values of greater than unity, and thus have very high dead volumes.

The behavior of the RTD curves changed completely after gas injection as depicted in Figures 2(a) and (b).

SAIKAT CHATTERJEE and KINNOR CHATTOPADHYAY are with the Process Metallurgy and Modelling Group, Department of Materials Science and Engineering, University of Toronto, 184 College Street, Toronto, ON, M5S 3E4 Canada. Contact e-mail: kinnor.chattopadhyay@utoronto.ca AMJAD ASAD, CHRISTOPH KRATZSCH, and RÜDIGER SCHWARZE are with the Institut für Mechanik und Fluidodynamik, Technische Universität Bergakademie Freiberg, Lampadiusstrasse 4, 09599 Freiberg, Germany.

Manuscript submitted August 8, 2016.

Article published online December 1, 2016.

The peak values of $C(\theta)$ for cases with gas injection are comparatively lower than those with no gas injection, suggesting decrease in dead volume fractions with increasing gas injections. The formation of bubble plume generates a lot of turbulence in the central part of tundish. The momentum of the bubble plume increases with increase in the gas injection. This strong convective flow near the shroud leads to a well-mixed region and consequently, decreases the dead volume fraction. Although the difference in $C(\theta)$ values between 6 and 10 pct cases is difficult to visualize from Figure 2(a), it can be observed clearly from Figure 2(b). The RTD curves for the inner and outer SENs are shown in Figures 2 (a) and (b), respectively. As the tracer took longer time to reach outer SENs, the peaks were formed at higher values of θ . Multiple peaks were observed for all the three RTD curves. This phenomenon is usually observed in the case of a bare tundish indicating the presence of a lot of short-circuiting flows.

The experimental data were analyzed using the correctly interpreted ‘modified mixing model’^[11] in order

to get better understanding of the flow field in the tundish by calculating the dead, mixed, and dispersed volume fractions. The calculated dead volume fractions are plotted for both the inner and outer SENs in Figure 3(a). The dead volume fraction for the inner SENs is seen to decrease rapidly with the increase in gas flow rate from 0 to 6 pct. However, the rate of decrease is sluggish when the gas flow rate increases from 6 to 10 pct. Since the flow direction of both the liquid and gas bubbles in the gas–liquid plume is vertical, increasing gas flow rate results in higher momentum of the plume in the vertical direction. The slow recirculating liquid elements are activated with the increase in gas flow rate, thus decreasing the dead volume fraction as shown in Figure 3(a). Although this behavior is noticed for the case of inner SENs, the same cannot be said for the outer SENs. Since the plume forms at a location far from the outer SENs, its effect on mixing near the outer SENs is negligible. The dead volume fraction was also noticed to decrease with increase in gas flow rate by Srivastava and Koria.^[6] The mixed volume fraction increases with the increase in gas flow rate for the case of

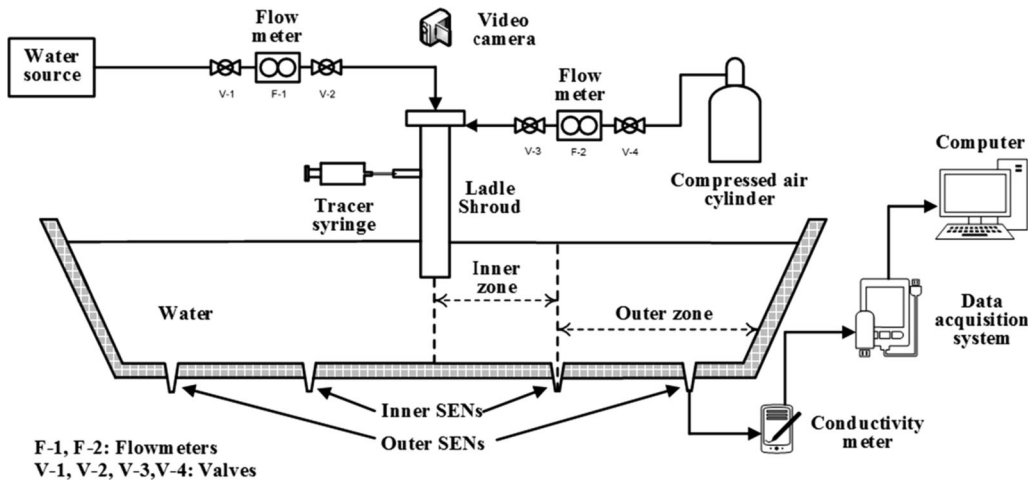


Fig. 1—Schematic diagram showing experimental setup for RTD measurements.

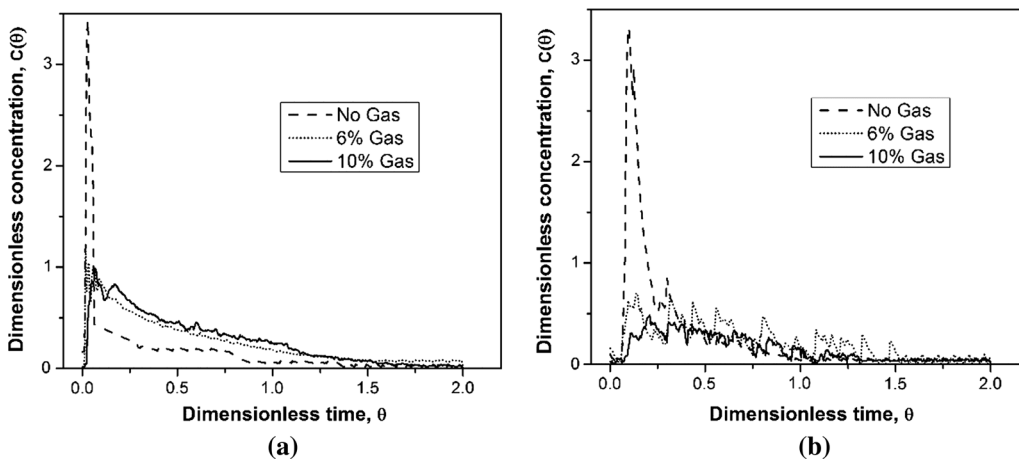


Fig. 2—Experimentally determined residence time distribution for (a) inner strands and (b) outer strands of tundish.

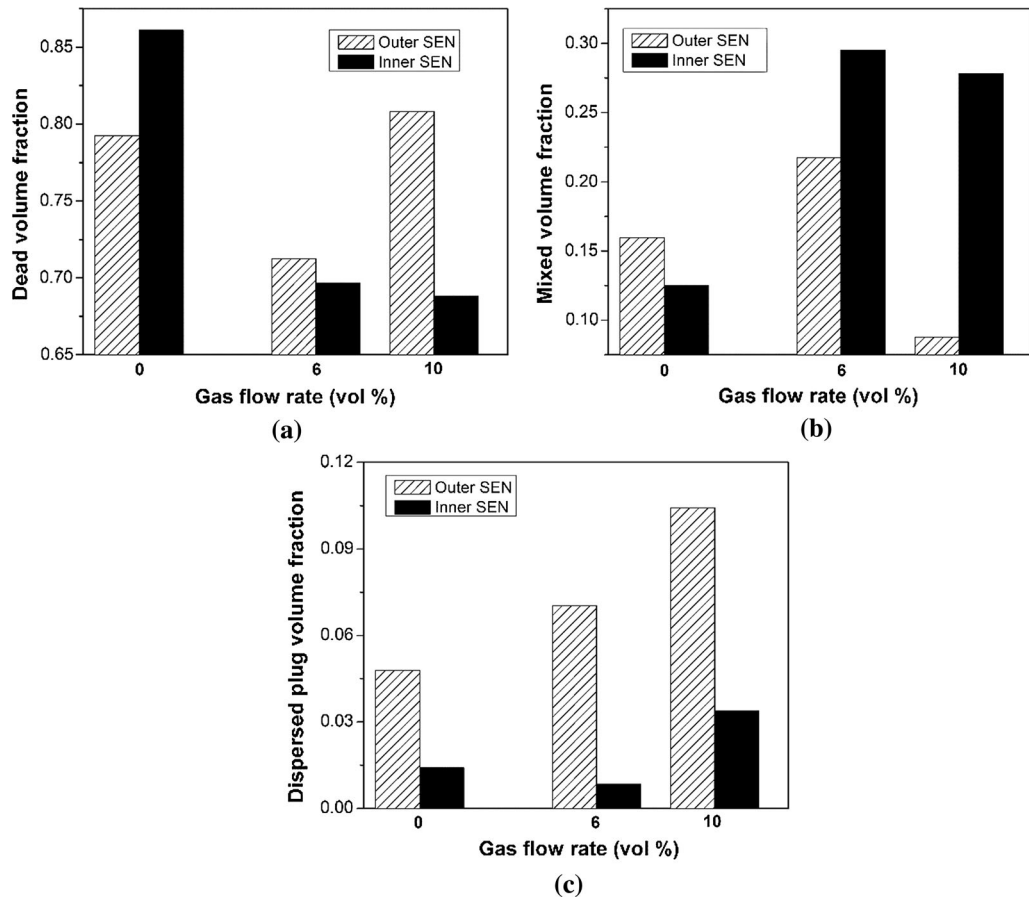


Fig. 3—Variation of (a) dead, (b) mixed, and (c) dispersed plug volume fractions with increasing gas flow rates.

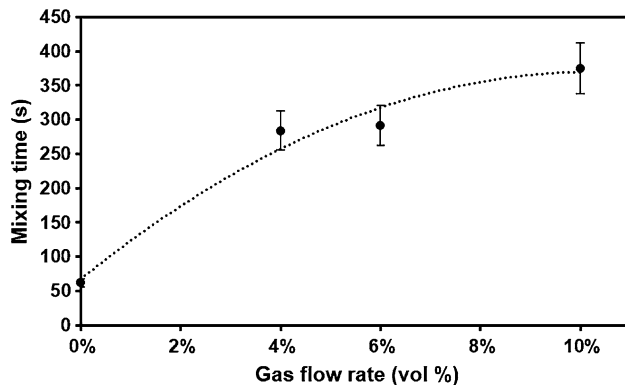


Fig. 4—Mixing time for various gas flow rates.

inner SENs as shown in Figure 3(b). This behavior can again be explained on the basis of good mixing near the plume region. Similar to the dead volume fraction, the mixed volume fraction did not show a specific trend for the case of outer SENs. Sahai and Ahuja^[1] had earlier reasoned that even though gas stream aided fluid mixing in the vertical direction, it acted as a barrier in the longitudinal direction. Hence, the tracer exiting from the plume region appeared as a vertically homogenized front. This vertical homogenization on account of

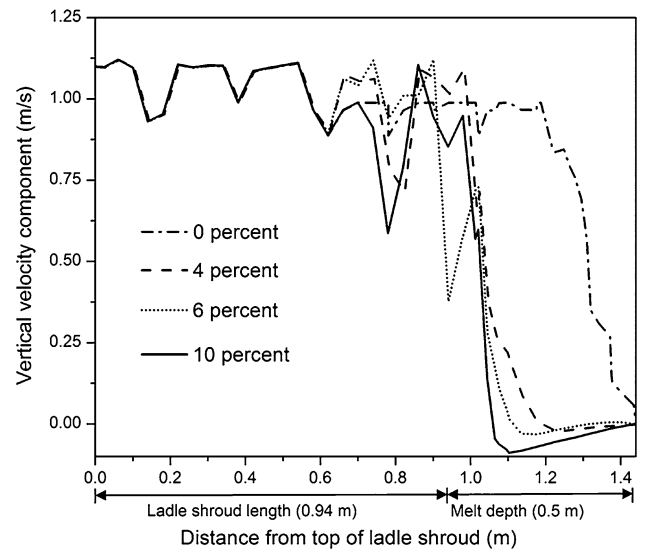


Fig. 5—Vertical component of the velocity at the center line through the ladle shroud.

turbulent plume movement affects mainly the inner SENs and not the outer ones.

Plug flow is defined as the type of flow where longitudinal mixing is non-existent. All the fluid elements have identical residence time in the tundish in the

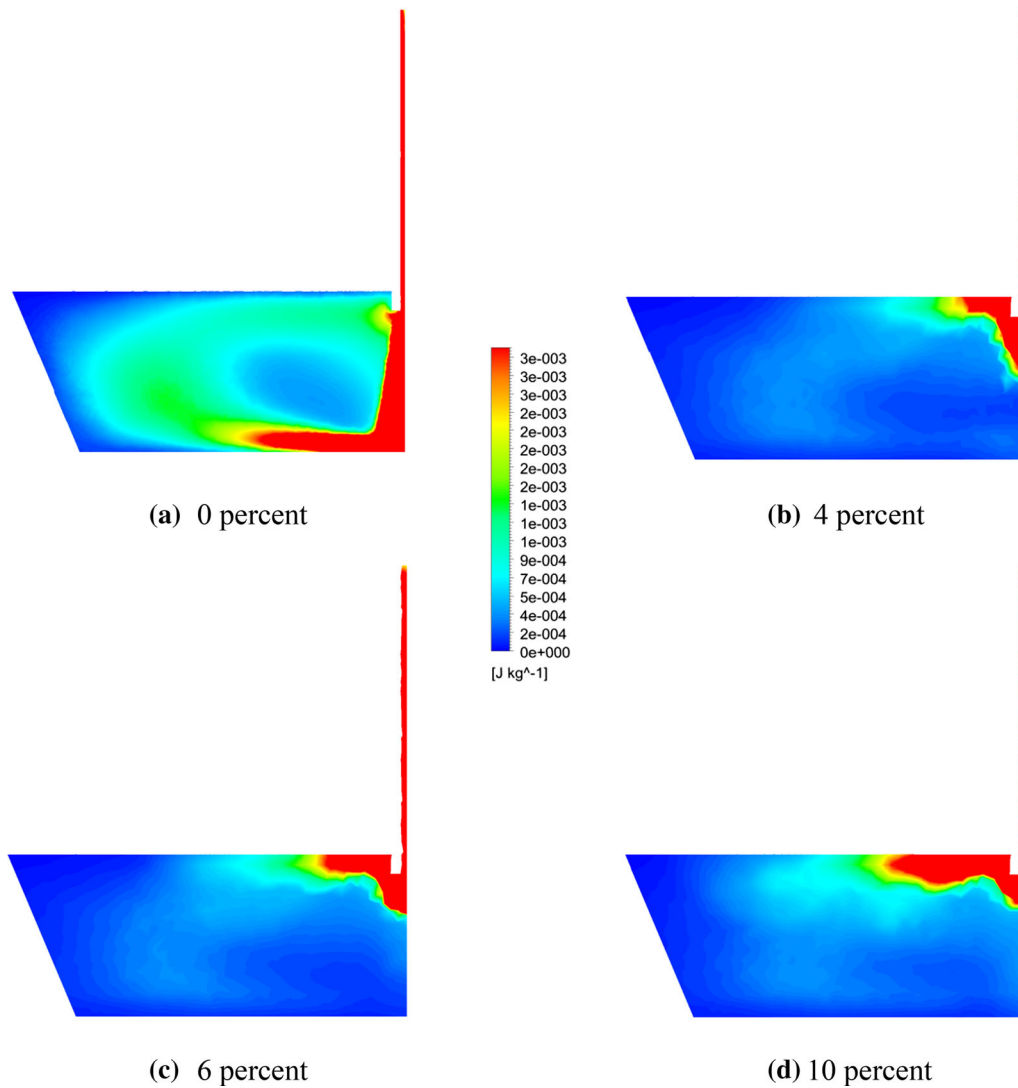


Fig. 6—Variation of turbulent kinetic energy at a vertical plane through inlet at different gas flow rates.

case of an ideal plug flow. The variation of dispersed plug flow volume fractions for both the inner and outer SENs are shown in Figure 3(c). There is a gradual increase with percent gas injection for both the cases of inner and outer SENs. Even though Srivastava and Korla^[6] found that there was no significant influence of gas flow rate on dispersed plug volume, Sahai and Ahuja^[1] noticed increase in dispersed plug volume with increasing gas flow rates. Since increase in gas injection enhances vertical homogenization without any longitudinal connection, plug flow volume fraction rises. Bubble plume acts as a barrier to longitudinal homogenization as flow direction inside the bubble plume is predominantly vertical. The rising gas bubbles make the flow surface-directed and thus, can be very helpful in flotation of inclusions. However, this also poses a threat of formation of open eyes^[7-9] which can be potential sites for heat loss, slag emulsification, reoxidation of liquid steel, and subsequent inclusion formation.

It is also interesting to see how the mixing time changes with different gas flow rates. The variation of

mixing time with gas injection is shown in Figure 4 below. Mixing time is the time taken by the tracer to diffuse completely in the longitudinal direction. Contrary to expectations, it is clearly seen that the mixing time in the tundish increases as the percentage of injected gas is increased. This is primarily because the gas bubble plume creates upwelling buoyant flows having negligible longitudinal component, and constrains the tracer in the 'inner zone' of the tundish (Figure 1). As a result, the tracer takes more time to diffuse longitudinally, thereby making the time of mixing longer. Mathematical modeling was performed to understand the behavior of the incoming jet and the distribution of turbulent kinetic energy (TKE) for various amounts of injected gas. The standard $k-\epsilon$ model of Launder and Spalding^[12] was used along with the Lagrangian discrete phase model^[13] to describe the turbulent bubbly flow inside the tundish. The gas injections were limited to 10 pct of water entry flows to ensure that the flow is in the bubbly range and large gas pocket formation is avoided. The vertical

component of the velocity along the center line of the shroud is depicted in Figure 5. The velocity was plotted from the top of the ladle shroud to the base of the tundish. For the case with no gas injection (0 pct), the vertical component of the jet velocity decelerates at about 50 pct of the melt depth. This is a result of an impinging jet event, where the vertical momentum is deflected into horizontal momentum, while the free jet attaches to the wall. Moreover, the jet loses some amount of vertical momentum by entrainment effects at the free shear layer, and thus increased spreading. Now as the gas injection percentages increase, the jet decelerates at about 10 to 20 pct of the melt depth. The upwelling gas plume counteracts the downward momentum of the jet and the resultant downward velocity decreases, becomes zero, and ultimately becomes negative at certain depths inside the melt, signifying entrainment into the buoyant jet. On examining the time-averaged TKE distribution in the central plane along the ladle shroud, as shown in Figure 6, it is clear that as the gas flow rate is increased, the TKE gets more and more concentrated near the free surface of the tundish as opposed to uniformly distributed in the whole tundish. This can explain why mixing of the tracer becomes slower at high gas flow rates. The mean velocity field is pushed more toward the slag layer with increasing gas injection, while turbulent mixing is still present near the shroud exit. Furthermore, mixing along a long distance of the flow streamlines is present in the cases with gas injection and is indicated by TKE contours in Figure 6.

Hence, it can be observed that the vertically activated plume enhances mixing in the ‘inner zone’ of the tundish and results in lower dead volume fraction and higher mixed and dispersed plug flow volume fractions. However, the ‘mixing time’ increases with gas injection as the longitudinal homogenization is blocked by the bubble plume. Hence, more work should be done to find out

alternative locations of inert gas injection which leads to decreased instead of increased mixing times.

NOMENCLATURE

$C(\theta)$	Dimensionless concentration
θ	Dimensionless time
c_i	Any concentration of tracer in the fluid at the vessel exit
c_{avg}	Average concentration of the tracer when it dissolves in the whole tundish fluid
RTD	Residence time distribution
TKE	Turbulent kinetic energy
SEN	Submerged entry nozzle

REFERENCES

1. Y. Sahai and R. Ahuja: *Ironmak. Steelmak.*, 1986, vol. 13, pp. 241–47.
2. D. Mazumdar and R.I.L. Guthrie: *ISIJ Int.*, 1999, vol. 39, pp. 524–47.
3. S. Singh and S.C. Koria: *ISIJ Int.*, 1993, vol. 33, pp. 1229–37.
4. G. Wang, M. Yun, C. Zhang, and G. Xiao: *ISIJ Int.*, 2015, vol. 55, pp. 984–92.
5. S. Chang, L. Zhong, and Z. Zou: *ISIJ Int.*, 2015, vol. 55, pp. 837–44.
6. S. Srivastava and S.C. Koria: *Scand. J. Metall.*, 1997, vol. 26, pp. 123–31.
7. S. Chatterjee and K. Chattopadhyay: *ISIJ Int.*, 2015, vol. 55, pp. 1416–24.
8. S. Chatterjee and K. Chattopadhyay: *Metall. Mater. Trans. B*, 2016, vol. 47B, pp. 508–21.
9. S. Chatterjee and K. Chattopadhyay: *Metall. Mater. Trans. B*, 2016, vol. 47B, pp. 3099–3114.
10. Y. Sahai and T. Emi: *Tundish Technology for Clean Steel Production*, World Scientific, Singapore, 2008, pp. 99–127.
11. Y. Sahai and T. Emi: *ISIJ Int.*, 1996, vol. 36, pp. 667–72.
12. B.E. Launder and D.B. Spalding: *Comput. Methods Appl. Mech. Eng.*, 1974, vol. 3, pp. 269–89.
13. Y.A. Buevich: *Fluid Dyn.*, 1966, vol. 1, p. 119.